Monthly Notices
of the
ROYAL ASTRONOMICAL SOCIETY

Mon. Not. R. Astron. Soc. **403,** 1317–1330 (2010) doi:10.1111/j.1365-2966.2009.16075.x

The properties of the stellar populations in ULIRGs – II. Star formation histories and evolution

J. Rodríguez Zaurín,[1,2]★ C. N. Tadhunter[2] and R. M. González Delgado[3]

[1]*Instituto de la Estructura de la Materia (CSIC), 28006, Madrid, Spain*
[2]*Department of Physics and Astronomy, University of Sheffield, Sheffield S3 7RH*
[3]*Instituto de Astrofisica de Andalucia (CSIC), PO Box 3004, 18080 Granada, Spain*

Accepted 2009 November 18. Received 2009 October 23; in original form 2009 April 3

ABSTRACT

This is the second of two papers presenting a detailed long-slit spectroscopic study of the stellar populations in a sample of 36 ultraluminous infrared galaxies (ULIRGs). In the previous paper, we presented the sample, the data and the spectral synthesis modelling. In this paper, we carry out a more detailed analysis of the modelling results, with the aim of investigating the general properties of the stellar populations (i.e. age, reddening and percentage contribution) and the evolution of the host galaxies, comparing the results with other studies of ULIRGs and star-forming galaxies in the high-z Universe. The characteristic age of the young stellar populations (YSPs) is $\leq$100 Myr in the nuclei of the overwhelming majority of galaxies, consistent with the characteristic time-scale of the major burst of star formation (SF) associated with the final stages of major galaxy mergers. However, the modelling results clearly reveal that the SF histories of ULIRGs are complex, with at least two epochs of SF activity. Overall, these results are consistent with models that predict an epoch of enhanced SF coinciding with the first peri-centre passage of the merging nuclei, along with a further, more intense, episode of SF occurring as the nuclei finally merge together. It is also found that, although YSPs make a major contribution to the optical emission in most of the extended and nuclear apertures examined, they tend to be younger and more reddened in the nuclear regions of the galaxies. This is in good agreement with the merger simulations, which predict that the bulk of the SF activity in the final stages of mergers will occur in the nuclear regions of the merging galaxies. In addition, our results show that ULIRGs have total stellar masses that are similar to, or smaller than, the break of the galaxy mass function (i.e. ULIRGs are sub-m_* or $\sim m_*$ systems), and that the YSPs detected at optical wavelengths dominate the stellar mass contents of the galaxies. Finally, we find no significant differences between the ages of the YSP in ULIRGs with and without optically detected Seyfert nuclei, nor between those with warm and cool mid- to far-IR colours. While these results do not entirely rule out the idea that cool ULIRGs with H II/LINER spectra evolve into warm ULIRGs with Seyfert-like spectra, it is clear that the active galactic nucleus (AGN) activity in local Seyfert-like ULIRGs has not been triggered for a substantial period ($\geq$100 Myr) *after* the major merger-induced starbursts in the nuclear regions.

Key words: galaxies: evolution – galaxies: starburst.

1 INTRODUCTION

First discovered in large numbers by the *IRAS* satellite, ultraluminous infrared galaxies (ULIRGs, $L_{\rm IR} > 10^{12}\,{\rm L}_{\odot}$) represent some of the most rapidly evolving objects in the local Universe. These objects are important in several respects, such as testing the merger models, investigating the nature of the active galactic nucleus (AGN)-starburst connection in merging systems and understanding the physical processes taking place in the recently discovered high-redshift star-forming galaxies, which have similar properties to the nearby ULIRGs.

A remarkable property of ULIRGs is that more than 90 per cent of them are associated with galaxy mergers and interactions (see Sanders & Mirabel 1996, for a review). The simulations have shown that, during galaxy collisions involving gas-rich disc galaxies, the gas loses angular momentum due to dynamical friction, tidal torques and inflows towards the centres of the galaxies (e.g. Mihos & Hernquist 1996). The resulting high nuclear concentrations of gas

★E-mail:jrz@damir.iem.csic.es

are capable of triggering both starburst and AGN activity. In general, these simulations predict two epochs of enhanced star formation (SF) in major galaxy mergers: the first occurring around the first peri-centre passage, and the second episode when the nuclei are close to coalescence (Barnes & Hernquist 1996; Mihos & Hernquist 1996; Springel, Di Mateo & Hernquist 2005; Cox et al. 2006; di Matteo et al. 2007; Cox et al. 2008). However, both the time lag and the relative intensity of the peaks of starburst activity during the merger event depend on several factors, such as the presence of bulges, feedback effects, gas content and orbital geometry. Given that the models make specific predictions about the histories of the SF triggered in the course of major gas-rich mergers, studies of the stellar populations in ULIRGs provide useful information about the mergers and, potentially, allow us to test the models.

ULIRGs are classified on the basis of their IR colours as warm ($f_{25}/f_{60} > 0.2$)[1] and cool ($f_{25}/f_{60} \leq 0.2$) ULIRGs. Warm ULIRGs represent ∼20–25 per cent of the total population of ULIRGs discovered by *IRAS*. Most such objects have an AGN optical spectral classification, tend to be more compact than cool ULIRGs, and are frequently found in an advanced merger state (Surace et al. 1998). These properties suggest that ULIRGs play an important role in the formation and evolution of quasi-stellar objects (QSOs) (Sanders et al. 1988b) and radio galaxies (Tadhunter et al. 2005). Indeed, Sanders et al. (1988b) proposed a scenario in which cool ULIRGs evolve into warm ULIRGs on their way to becoming typical optically selected QSOs. Further evidence in favour of such an evolutionary scenario was reported by Surace et al. (1998), Surace & Sanders (1999), Surace, Sanders & Evans (2000) and Surace & Sanders (2000) on the basis of their imaging studies of cool and warm ULIRGs, and Canalizo & Stockton (2000a,b), 2001), based on a spectroscopic analysis of a sample of transition QSOs – objects that, based on their IR colors, may represent a transitionary stage between ULIRGs and QSOs. More recently, Tadhunter et al. (2007) carried out a mid- to far-IR study of powerful radio galaxies, searching for signs of hidden SF activity. They found that the fraction of powerful radio galaxies with energetically significant SF activity (20–30 per cent) is similar to that deduced from optical studies. The derived ages and masses of the young stellar populations (YSPs) are consistent with the idea that some radio galaxies are the evolved products of ULIRGs (Tadhunter et al. 2005; Willis et al. 2008).

In terms of the end products of the merger events associated with ULIRGs, the kinematic studies of Genzel et al. (2001) and Tacconi et al. (2002) have shown that ULIRGs match the locations of intermediate mass, discy ellipticals and S0 galaxies in the fundamental plane. ULIRGs have effective radii and velocity dispersions smaller than those of their comparison sample of nearby radio galaxies. Furthermore, the dynamical masses of ULIRGs are 10^{10}–10^{11} $M_{\odot}$ (Tacconi et al. 2002; Colina, Arribas & Monreal-Ibero 2005; Dasyra et al. 2006a,b), which is similar to intermediate-mass elliptical galaxies. Based on the dynamical properties of ULIRGs, Tacconi et al. (2002) concluded that not all ULIRGs can evolve into typical QSOs or powerful radio galaxies. However, the recent work of Dasyra et al. (2007), based on near-IR spectroscopic observations of a sample of 12 (mainly Palomar Green) QSOs, has shown that it is possible for ULIRGs to have similar dynamical properties to QSOs. Therefore, it is clear that, despite the recognition of an evolutionary link between ULIRGs, QSOs/radio galaxies and elliptical galaxies, considerable uncertainties remain about the true nature of the link.

[1] The quantities f_{25} and f_{60} represent the *IRAS* flux densities in Janskys at 25 and 60 μm.

Studies of ULIRGs are also important in the context of the various populations of high-z galaxies that have been recently detected using near-IR [distant red galaxies (DRGs); Franx et al. 2003], mid-IR (24 μm *Spitzer*-selected galaxies; Caputi et al. 2006; Sajina et al. 2007; Yan et al. 2007, and others) and submillimetre (sub-mm) wavelengths [sub-mm galaxies (SMGs); Chapman et al. 2003, Pope et al. 2005, and others]. These objects have properties similar to the nearby ULIRGs (stellar mass and luminosity, for example), and make up a substantial fraction of the SF rate density at $z \sim 1$–2 (Pérez-González et al. 2005). As local analogues of such objects, ULIRGs provide an opportunity to study the physical processes associated with their prodigious SF activity in depth.

It is also important to emphasize that most of the studies of the stellar populations in high-redshift galaxies are based on the modelling of a few photometric points and, therefore, it is hard to constrain the properties of these populations. Sensitive studies of star-forming galaxies at lower redshifts are useful, not only to better understand the links between local starburst objects and their high-z counterparts, but also to gain valuable information on the uncertainties associated with the derived properties of the stellar populations in high-z star-forming galaxies.

At this stage, it is clear that there are many unresolved issues concerning the nature of ULIRGs. In particular, we emphasize the following key questions.

(i) Do the merger simulations adequately describe the observed properties of ULIRGs?

(ii) Do the properties of the stellar populations in ULIRGs correlate with other properties of ULIRGs, such as IR luminosity, interaction class or spectral classification?

(iii) What is the nature of the links between ULIRGs and other types of object in the local universe, such as QSOs, radio galaxies and elliptical galaxies?

Given their importance for studying the evolution of galaxies via major gar-rich mergers, it is perhaps surprising that there have been relatively few studies of stellar populations in ULIRGs. Many previous studies have concentrated on studying the SEDs and mid-IR emission-line spectra of ULIRGs, with an emphasis on determining the dominant heating mechanism for the mid- to far-infrared (MFIR)-emitting dust (e.g. Farrah et al. 2003). However, such studies are not capable of determining the detailed properties of the stellar populations and how they vary with spatial location in these complex systems. Therefore, in order to address the key issues surrounding the evolution of ULIRGs, we have undertaken a programme of deep optical long-slit spectroscopic observations of a substantial sample of nearby ULIRGs, aimed at investigating their SF histories. In Rodríguez Zaurín et al. (2009), hereafter Paper I, we presented the sample, data reduction and spectral synthesis modelling techniques. In this paper, we discuss the results presented in Paper I in the context of evolutionary models for merging systems and the results obtained from studies of stellar populations in high-z star-forming galaxies.

Throughout this paper, we assume a cosmology with $H_0 = 71\,\mathrm{km\,s^{-1}\,Mpc^{-1}}$, $\Omega_0 = 0.27$, $\Omega_\Lambda = 0.73$.

2 MODELLING THE STELLAR POPULATIONS: GENERAL RESULTS

In Paper I, we presented the results of spectral synthesis modelling of the complete (CS) and the extended (ES) samples, including 26 and 36 ULIRGs, respectively. The detailed properties of these samples are described in that paper. To summarize, in the first place,

we observed a complete RA-limited and Dec.-limited subsample of the Kim & Sanders (1998) 1 Jy sample of ULIRGs, with RAs in the range $12 < \mathrm{RA} < 1{:}30$ h, declinations $\delta > -23^{\circ}$ and redshifts $z < 0.13$. The redshift limit was chosen to ensure that the objects are sufficiently bright for spectroscopic study, and also to keep the size of the sample tractable for deep observations on 4-m class telescopes. We will refer to this sample of 26 objects as the CS (see table 1 in Paper I for details of some of the properties of the ULIRGs in the CS). In addition, we also observed 10 objects outside the redshift range and/or the RA and Dec. range of the CS. With the aim of including a larger number of warm objects (only eight warm ULIRGs are included in the CS), seven of these 10 ULIRGs have warm mid- to far-IR colours. The sample including the CS and these 10 additional objects will be referred to as the ES. Thus, the ES comprises 36 objects: 21 cool ULIRGs and 15 warm ULIRGs. Since the ES accounts better for the diversity within the ULIRG phenomenon, and our statistical analysis shows no significant differences between the properties of the stellar populations in the ES and CS, we concentrate on the ES sample for the study presented in this paper.

In order to perform a detailed study of the stellar populations in ULIRGs, a total of 133 apertures was extracted for the objects in the ES. The extraction apertures were selected from spatial cuts of the 2D frames in the line-free continuum wavelength range 4400–4600 Å, based on the visible extended structures and the requirement that the apertures are large enough to have a sufficiently high S/N ratio for further analysis. To compare the stellar populations between the objects in our sample, apertures with a metrical scale of 5 kpc centred on the main nuclei were extracted for all the objects in the ES, including separate extractions for multiple nuclei in individual sources. A second set of apertures was then selected to sample the spatial features of those objects in the ES showing tails, bridges and other diffuse structures.

To perform the fits, we have used the CONFIT code (see Robinson et al. 2000 and Rodríguez Zaurín, Tadhunter & González Delgado 2008, hereafter RZ08). The CONFIT approach consists of a direct fit of the overall continuum shape of the extracted spectra using on a minimum χ^2 technique (Tadhunter et al. 2005; Rodríguez Zaurín et al. 2007, hereafter RZ07). CONFIT is based on a 'simplest model' approach, i.e. we fit the minimum number of stellar components required to adequately model the data. Therefore, CONFIT allows for a maximum of two stellar components plus a power law in some cases. Throughout this paper, we define YSPs as stellar components with ages $t_{\mathrm{YSP}} \leq 2$ Gyr, and old stellar populations (OSPs) as components with ages $t_{\mathrm{OSP}} > 2$ Gyr. With the aim of better describing each combination, it is convenient to further subdivide the YSPs into two groups: very young stellar populations (VYSPs), stellar components with ages $t_{\mathrm{VYSP}} \leq 0.1$ Gyr; intermediate-age young stellar populations (IYSP), stellar components with ages in the range of $0.1 < t_{\mathrm{IYSP}} \leq 2$ Gyr.

Given that the properties of the stellar populations were not known a priori, three modelling combinations were investigated. The results obtained for each of the combinations are described in detail in Paper I, and are summarized as follows.

(i) *Combination I.* As a first approach, we used a two-component model comprising a YSP ($t_{\mathrm{YSP}} \leq 2$ Gyr) with varying reddening [$0.0 \leq E(B-V) \leq 2.0$, increasing in steps of 0.1], along with an unreddened OSP of age 12.5 Gyr. Accounting for an old component covers the case in which one or more of the merging galaxies is early-type or bulge-dominated galaxy. Using this combination, we obtained adequate fits ($\chi^2_{\mathrm{red}} \leq 1.0$) to the overall shape of the SED for all but one (IRAS 23060+0505, for which a power law is required) of the extraction apertures modelled. However, Combination I fails to adequately fit the detailed absorption features – particularly, the Ca II K feature – for ∼42 per cent (54) of the apertures modelled.[2]

(ii) *Combination II.* This combination consists of three components: an OSP of age 12.5 Gyr and zero reddening, along with a YSP with variable reddening [$0.0 \leq E(B-V) \leq 2.0$, increasing in steps of 0.1], and a power law with a spectral index in the range $-15 < \alpha < 15$. The power law is included to represent either scattered or direct AGN continuum component (Tadhunter et al. 2002), or a highly reddened VYSP. Adequate fits ($\chi^2 \leq 1.0$) to the overall SED shapes were found for all of the apertures of all objects using this combination. On the other hand, this combination fails to fit the detailed absorption features for 10 per cent (13 apertures) of the apertures modelled. We find that the minimum percentage contribution of the OSP component is less that 10 per cent (due to the uncertainties inherent in the modelling techniques percentage contributions <10 per cent are considered negligible) for most of the apertures. This result suggests that an OSP component is not required to fit the optical spectra of the majority of the objects in the ES.

(iii) *Combination III.* A drawback of Combination II is that, for those cases in which the power law is likely to represent a VYSP component, it gives no information about the detailed properties (age and reddening) of such a component. In addition, for ULIRGs as a class, there is no reason, a priori, to expect a major contribution to the optical emission from a 12.5 Gyr OSP. Such lack of an OSP is also suggested by the results of Combination II. Therefore, in order to explore the possibility of YSPs dominating the optical emission from the objects, we used a combination consisting of two YSP components: a IYSP with ages in the range of 0.3–2.0 Gyr, with $E(B-V)$ values of 0.0, 0.2 or 0.4, plus a VYSP with age in the range of 1–100 Myr and reddenings $0.0 \leq E(B-V) \leq 2.0$ (increasing in steps of 0.1). Adequate fits to both the continuum and the detailed absorption features are obtained for all but 9 (∼7 per cent) of the extraction apertures modelled. In the minority of the cases for which no adequate fits could be obtained using Combination III, either an OSP or a power-law component was required in addition to a YSP.

Significantly, for the majority of apertures, we find that both the SEDs and the detailed absorption features can be adequately modelled with all three combinations, although in most cases Combination III provides the best overall fit. This demonstrates that it can be difficult to derive a unique model solution even with high-quality, wide spectral coverage optical spectra. None the less, the fits provide the following general results.

(i) *Dominant young stellar populations.* YSPs dominate the optical light, while OSPs are relatively unimportant, in the overwhelming majority of apertures modelled. In terms of the nuclear apertures, the only exceptions are IRAS 13451+1232 5kpc, IRAS 1648NE 5kpc, IRAS 21208−0519 5kpcII, IRAS 23233+2817 5kpc and IRAS 23327+2913 5kpcII. Although there is some ambiguity in the cases of IRAS 13451+1232 5kpc, IRAS 1648NE 5kpc and IRAS 23233+2817 5kpc which can be modelled either in terms of a dominant OSP plus a YSP (Combination I) or a dominant 'old' IYSP (>1 Gyr) plus a VYSP (Combination III), we can only adequately model IRAS 21208−0519 5kpcII and IRAS 23327+2913 5kpcII with Combination I models that include an

[2] As discussed in Paper I, some of this discrepancy may be due to the effect of interstellar medium (ISM) absorption on the Ca II K resonance line.

OSP. Note that, in the case of IRAS 23327+2913 5kpcII, it is possible to model the optical spectrum using an OSP, without any requirement for a YSP. Apart from these exceptions, for most objects the results are consistent with the idea that the precursor galaxies are gas-rich spiral galaxies.

(ii) *Complex star formation histories.* Consistent with our previous results for the nearby ULIRG Arp220 (RZ08), we find that most apertures of most objects are best-fitted with models that include a combination of VYSP and IYSP (i.e. Combination III). This suggests that the recent SF histories of most ULIRGs are complex, with at least two SF epochs, even if the most recent (represented by the VYSPs) often dominates the optical light.

In the following sections, we consider the properties of the YSP in ULIRGs in more quantitative detail, and investigate whether they are correlated with other properties of these merging systems.

2.1 Characteristic properties of the YSPs in the nuclear and extended regions

As described in Paper I, Combination I (YSP + OSP) provides useful estimates of the 'luminosity weighted' ages (LW ages), reddenings and percentage contributions of the dominant YSPs within each galaxy. Providing a single estimate (with an associated uncertainty) for the parameters associated with the YSPs in each aperture, this combination is particularly useful for performing a statistical analysis of the properties of the stellar populations in the CS and the ES samples.

Fig. 1 shows the distributions of the average LW ages, reddenings [LW-$E(B-V)$] and percentage contributions to the flux in the normalizing bin (LW per cent) of the YSPs in the nuclear and extended apertures. This figure has been made using 34 of the 36 objects in the ES. For two of the three objects classified as Sy1

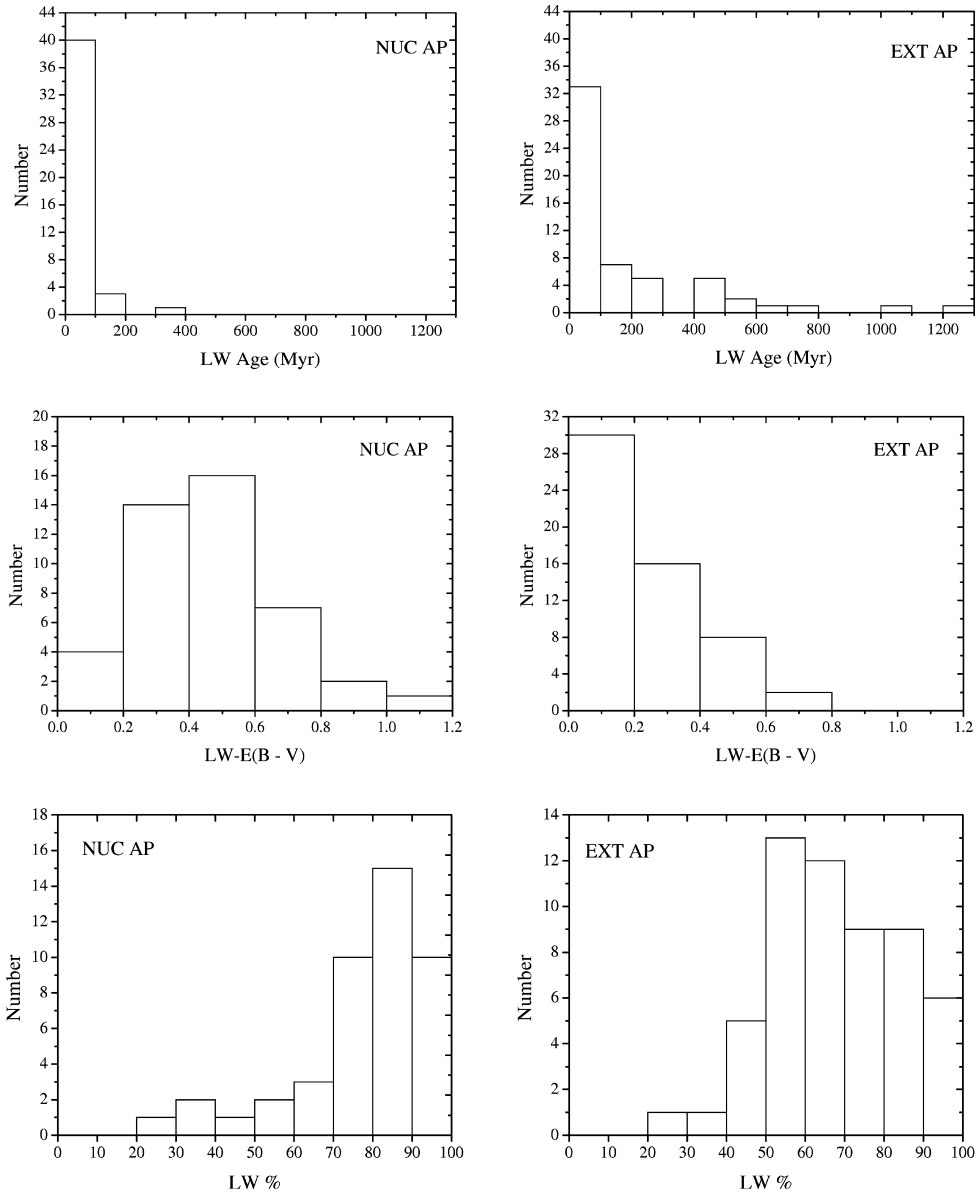

Figure 1. Histograms showing the LW age (top), LW-$E(B-V)$ (middle) and LW per cent (bottom) contribution distributions for the nuclear 5 kpc (left) and the extended (right) apertures. The results of Combination I show that YSPs are present at all locations in the galaxies for the majority of the objects in the ES, with a clear cut-off in YSP ages at 100 Myr in the case of the nuclear regions. The figure also suggests that the YSPs in the nuclear regions of the galaxies, coinciding with higher reddening, make a larger contribution to the flux at optical wavelengths than those in the extended regions.

Table 1. Mean and median values for the parameters associated with the YSPs for both the nuclear and extended regions of the objects in the ES, obtained using Combination I.

		Mean	Median
NUC AP	LW age (Myr)	66	60
	LW-$E(B-V)$	0.4	0.4
	LW per cent	77	82
EXT AP	LW age (Myr)	203	80
	LW-$E(B-V)$	0.2	0.2
	LW per cent	63	66

Table 2. Results of the K–S test for the significance of differences between the distributions in the nuclear and the extended regions, of the LW age, LW-$E(B-V)$ and LW per cent for the ES and using Combination I.

	D	Confidence level
LW age	0.325	99 per cent
LW-$E(B-V)$	0.50	$>$ 99.9 per cent
LW per cent	0.383	$>$ 99.9 per cent

Note. Column (2): the maximum deviation between the two cumulative distribution functions. Column (3): the probability that the difference between the distribution of the nuclear and the extended regions is significant.

(IRAS 15462−0450 and IRAS 21219−1757) no extended apertures were extracted and, therefore, they are not included in the analysis presented here. In the case that one of the extended apertures samples a similar region to the 5 kpc aperture, only the latter is used for the plots (e.g. ApE and 5 kpc in the case of Mrk 273). In the case of Arp 220, only two of the 24 apertures were included, in order to avoid giving too much weight to the extended apertures in a single object. These are the 5 kpc aperture and $\mathrm{AP_{TOTAL}}$ for PA 75°. Overall, a total of 100 of the 128 apertures modelled for the ES were eventually used for the figures.

The upper panel of Fig. 1 shows the presence of a clear upper limit of 100 Myr for the LW ages of the YSPs in the nuclear apertures; only 9 per cent of the nuclear apertures (4 of the 44 nuclear apertures used) have average LW ages older than this value. In contrast, 41 per cent of the extended apertures (23 of the 56 extended apertures used) have average LW age values older than 100 Myr, and as old as 1.2 Gyr. In terms of reddening, Fig. 1 (middle) suggests the presence of higher reddening [LW-$E(B-V)$] values in the nuclear regions of the galaxies compared with the extended regions. We also find that the YSPs represent the dominant contribution (LW per cent $\geq$ 50 per cent) to the optical emission for all but 11 (11 per cent) of the apertures used (four nuclear apertures and seven extended apertures; Fig. 1, bottom panel). However, the YSPs tend to make a larger contribution to the optical light in the nuclear regions.

Table 1 shows the mean and median values of the different parameters associated with the YSPs. To investigate whether the distributions of the YSPs properties in the nuclear and extended regions are indeed different, we used the Kolmogorov–Smirnov (K–S) two-sample test, and the results are presented in Table 2. We find that the differences between the LW age, LW-$E(B-V)$ and LW per cent distributions for the YSPs in the nuclear and extended regions of the galaxies are significant with a confidence level of $\gtrsim$99 per cent (i.e. the probability that the distributions are drawn at random from the same parent distribution is $<$1 per cent).

To further investigate the properties of the stellar populations, we performed a similar study to that presented above using the results of Combination III (VYSP + IYSP). Fig. 2 shows the distributions of the average values for the VYSPs age, reddening and the minimum percentage contribution to the flux in the normalizing bin ($P^{\mathrm{min}}_{\mathrm{VYSP}}$), for both the nuclear and the extended regions. From a visual inspection of the histograms, the modelling results suggest the presence of 'younger' and more reddened VYSPs in the nuclear regions of the objects. Moreover, the lower panel in Fig. 2 is designed to show the importance of the VYSPs within the different regions of the galaxies sampled by the apertures. The figure suggests that VYSPs are more important in the nuclear regions of the galaxies. Table 3 presents the mean and median values for the VYSP age, VYSP-$E(B-V)$ and $P^{\mathrm{min}}_{\mathrm{VYSP}}$, while Table 4 shows the results of the K–S test obtained using Combination III. We find that the difference between the VYSPs age and $E(B-V)$ distributions in the nuclear and the extended regions is significant with a confidence level of 95 per cent. In the case of $P^{\mathrm{min}}_{\mathrm{VYSP}}$, the confidence level is 99.5 per cent. Overall, the results are consistent with those of Combination I, but the level of significance is lower.

The lower panel of Fig. 2 also shows the locations of IRAS 13451+1232 (PKS 1345+12) and Arp 220, the two objects for which detailed studies were presented in RZ07 and RZ08. Arp 220 is frequently used as the archetype of ULIRGs as a class. However, the modelling results indicate that the YSPs in this object are not typical of ULIRGs in general. While significant VYSPs are detected at all locations of the galaxies sampled by the apertures, in the case of Arp 220 the contribution of such populations is relatively small, apart from in the nuclear region of the galaxy. Furthermore, in this object, a uniform IYSP of age 0.5–0.9 Gyr is found at all locations sampled by the apertures.

In the case of PKS 1345+12, some peculiarities might be expected, since this is the only object in our sample classified as radio galaxy. For this object, either OSPs or dominant 'old' IYSPs (1–2 Gyr) are required to model the data (see Paper I for details); the contribution from VYSPs is relatively small. Independent of the combination of stellar populations assumed, this galaxy is the most massive amongst the objects in our sample (see table 4 in Paper I).

Overall, our modelling results indicate that the VYSPs in the nuclear regions of the ULIRGs make a more significant contribution to the optical light than those of the extended regions. In terms of age and reddening, the VYSPs located in the nuclear regions tend to be younger and more reddened. These results will be discussed in the context of the merger simulations in Section 6.

2.2 Correlations between the properties of the YSP and other ULIRG properties

Given that certain of the general properties of ULIRGs (e.g. IR luminosities, mid- to far-IR colours, optical morphology and spectral class) may change as the systems evolve along the merger sequence, it is interesting to investigate whether such properties correlate with those of the YSP deduced from spectral synthesis modelling.

With the aim of determining whether the more luminous objects have younger, redder or more significant VYSPs, Fig. 3 shows the average VYSP age, reddening [$E(B-V)$] and minimum percentage contribution ($P^{\mathrm{min}}_{\mathrm{VYSP}}$) obtained for the nuclear 5 kpc apertures, plotted against the log of the IR luminosity (from Kim & Sanders 1998). Note that, since it was not possible to model the Sy1-ULIRGs (IRAS 12540+5708, IRAS 15462−0450 and IRAS 21219−1757, see Paper I for details), no Sy1 galaxies are shown in

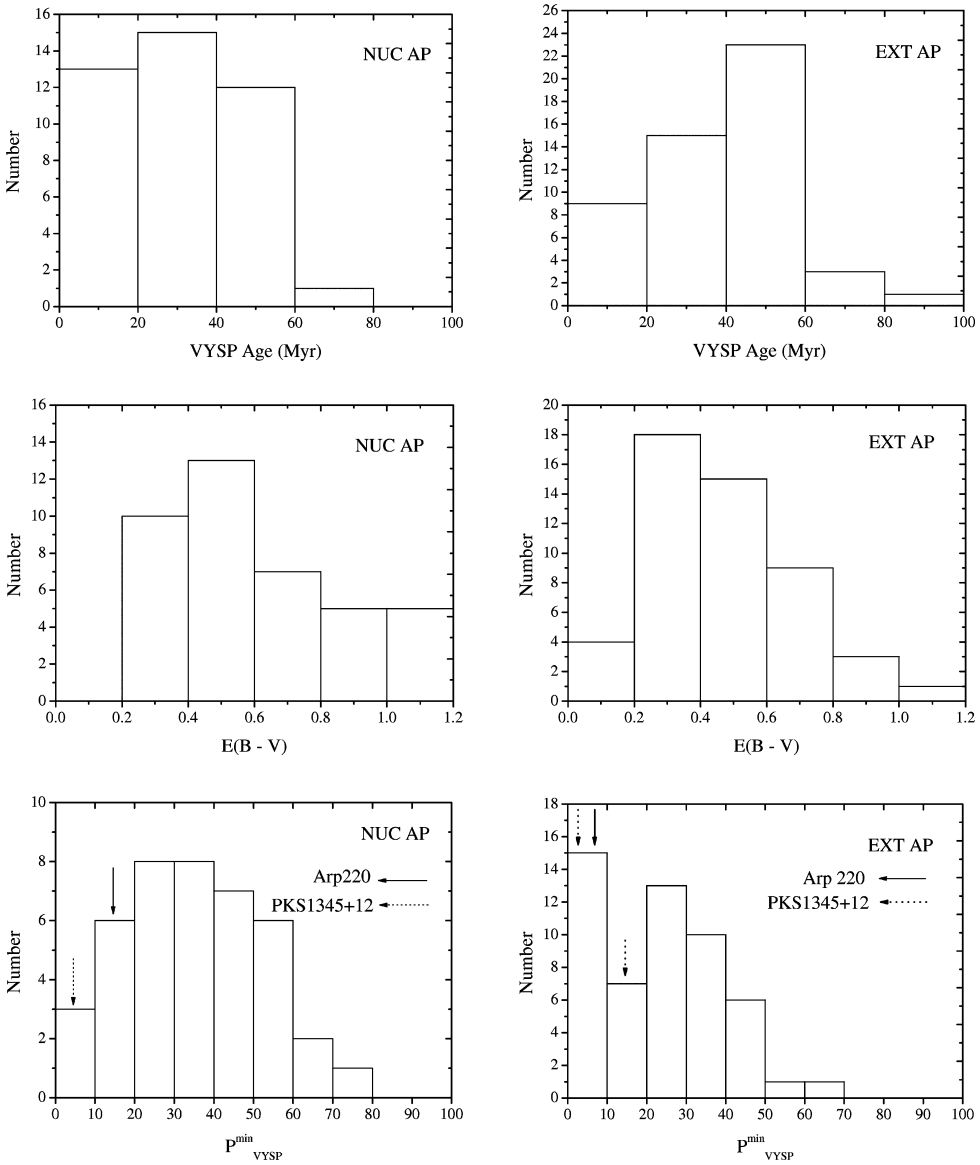

Figure 2. Histograms showing the distributions of the average VYSP age (top), $E(B-V)$ values (middle) and the minimum percentage contribution to the flux in the normalizing bin ($P^{\rm min}_{\rm VYSP}$, bottom) for the nuclear 5 kpc (left) and the extended (right) apertures, using the ES and Combination III. The locations of Arp 220 and PKS1345+12 are also shown in the figure.

Table 3. Mean and median values for the parameters associated with the VYSPs, for both the nuclear and extended regions of the objects in the ES, obtained using Combination III.

		Mean	Median
NUC AP	VYSP age (Myr)	31	30
	VYSP-$E(B-V)$	0.6	0.6
	$P^{\rm min}_{\rm VYSP}$	37	39
EXT AP	VYSP age (Myr)	39	50
	VYSP-$E(B-V)$	0.4	0.4
	$P^{\rm min}_{\rm VYSP}$	24	25

Table 4. Results of the K–S test for the significance of differences between the distributions in the nuclear and the extended regions, of the VYSP age, VYSP-$E(B-V)$ and $P^{\rm min}_{\rm VYSP}$ for the ES, using Combination III.

	D	Confidence level
VYSP age (Myr)	0.27	95 per cent
VYSP-$E(B-V)$	0.27	95 per cent
$P^{\rm min}_{\rm VYSP}$	0.35	99.5 per cent

Note. Column (2): the maximum deviation between the cumulative distribution functions. Column (3): the probability that the difference between the distribution of the nuclear and the extended regions is significant.

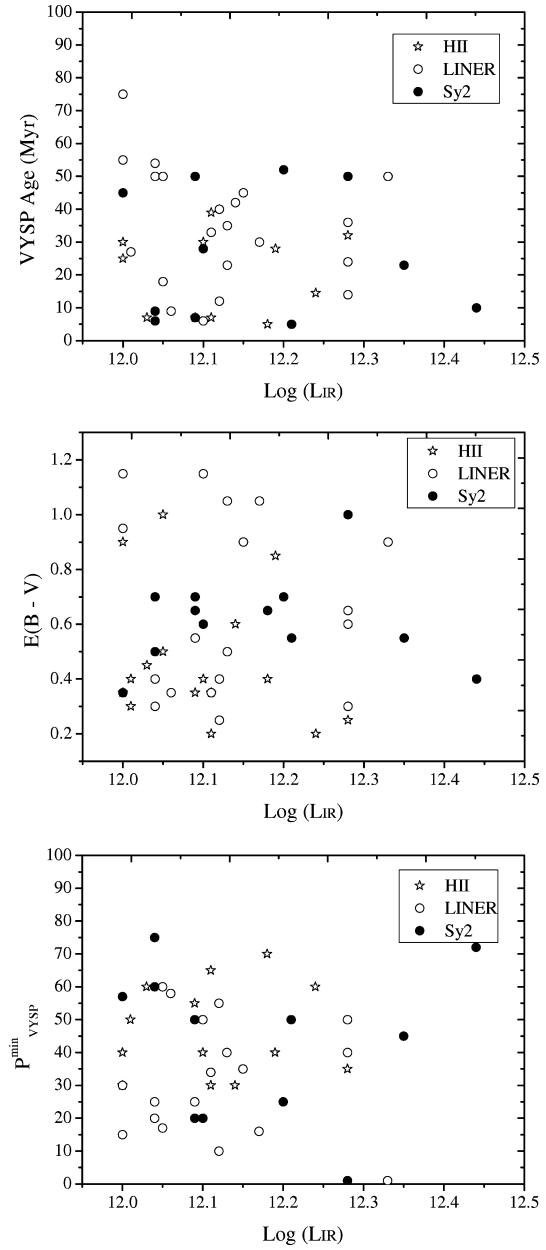

Figure 3. Average VYSP age, $E(B-V)$, and $P^{\rm min}_{\rm VYSP}$ plotted against Log($L_{\rm IR}$). The nuclear 5 kpc apertures have been used for these plots. The points are labelled based on the Veilleux et al. (1999) spectral classifications. No significant correlations are observed.

the figure. We find that the properties of the VYSPs are independent of the IR luminosities of the sources.

In addition to looking for trends with luminosity, we can also examine whether the stellar properties depend on the optical spectral classification. As can be seen from Fig. 3, where the points are labelled according to spectral classification, we see no clear trend with optical type. Table 5 shows the mean and median values of the VYSP age, reddening and $P^{\rm min}_{\rm VYSP}$ for the different types of objects, i.e. H II-, LINER- and Sy2-ULIRGs. If, for example, there exists an evolutionary link between the H II- or LINER-ULIRGs and the Sy2-ULIRGs (Sanders et al. 1988b), the latter representing a more advanced stage in an evolutionary sequence, one might expect the Sy2-ULIRGs to have older ages. No trends are apparent in Fig. 3 for the different spectral types of ULIRGs. A first interpretation is

Table 5. Mean and median values of the VYSP age, VYSP-$E(B-V)$ and $P^{\rm min}_{\rm VYSP}$ for the H II, LINER and Sy2-ULIRGs, for the nuclear 5 kpc apertures.

		Mean	Median
H II	VYSP age (Myr)	20	25
	VYSP-$E(B-V)$	0.5	0.4
	$P^{\rm min}_{\rm VYSP}$	46	40
LINER	VYSP age (Myr)	35	35
	VYSP-$E(B-V)$	0.6	0.6
	$P^{\rm min}_{\rm VYSP}$	34	34
Sy2	VYSP age (Myr)	28	25
	VYSP-$E(B-V)$	0.6	0.6
	$P^{\rm min}_{\rm VYSP}$	43	50

that there is no evolutionary link between H II-, LINER- and Sy2-ULIRGs. However, it is also possible that the transition between one type and the other occurs over a shorter time-scale than the typical time-scale of the enhancement of the SF activity in the final stages of the merger event as the nuclei coalesce (∼100 Myr, Barnes & Hernquist 1996). In that case, no trend is expected to be observed.

We have also investigated the presence of correlations between the properties of the VYSPs and other properties of ULIRGs such as the Veilleux, Kim & Sanders (2002) interaction class, or the MFIR colour ratio f_{25}/f_{60}. The conclusions reached are identical, i.e. no evidence for correlations or trends is found.

As well as the explanation already discussed above, possible reasons for the lack of correlations between the YSP properties and other properties of ULIRGs include the following.

(i) *Selection effect*. Since the objects in the CS and the ES samples are ULIRGs, with high IR luminosities and SF rates, it is likely that we are observing them at, or after, the first peri-centre passage, or at the end of the merger event, when the nuclei are very close to coalescing. Therefore, they all have similar properties.

(ii) *Modelling technique*. The outputs of the modelling technique used for the analysis presented in this section, as described in detail in Paper I, are ranges of age, reddening and percentage contribution of both IYSPs and VYSPs. Therefore, part of the scatter in the YSP properties could be due to the uncertainties inherent in the modelling technique; such uncertainties could hide underlying trends and patterns in behaviour.

(iii) *Other variables*. There are other variables such as, for example, the gas contents of the parent galaxies or the geometry of the merger, that could have a more important impact on the properties of the VYSPs in ULIRGs than the spectral classification, MFIR colours, MFIR luminosities or the interaction class.

Interestingly, this apparent lack of correlations between the various properties of ULIRGs has been found by other authors. Veilleux, Kim & Sanders (1999) found no correlation between the emission-line reddenings and other properties of ULIRGs, such as the MFIR colour ratio f_{25}/f_{60}, for the 108 objects in their sample. Moreover, Farrah et al. (2001) carried out an *HST*-WFPC2 V-band imaging study of a sample of 23 ULIRGs and found no correlation between the IR luminosities and the morphologies of the objects in their sample.

3 THE MASSES OF THE YSPs

Table 4 in Paper I presents estimates of the total stellar masses associated with the different stellar components for the objects in the

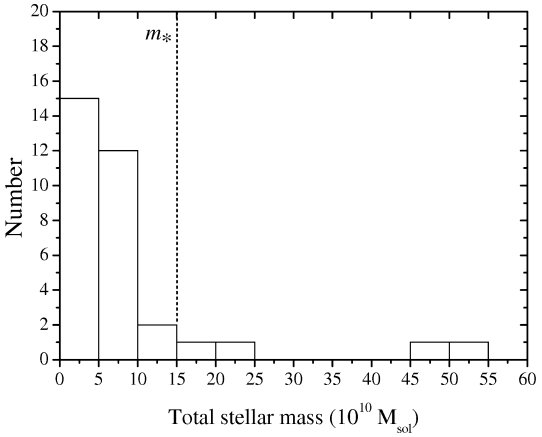

Figure 4. Histogram showing the distribution of the total stellar mass values presented in Table 6 for the objects in the ES. The figure shows that only six of the objects have stellar masses $M_{\rm stellar} > 1 \times 10^{11}\,{\rm M}_{\odot}$.

ES. Fig. 4 shows the distribution of the total stellar masses presented in that table [accounting for all VYSP, IYSP and OSP (if present)]. Note that, in the cases of IRAS 14394+5332, IRAS 17028+5817 and IRAS 23327+2913, the total stellar mass was estimated for the two nuclei individually and, for the purpose of the figure, the masses of the two nuclei were added. The figure shows that only six objects in our sample – IRAS 00188−0856, IRAS 13451+132, IRAS 14348−1447, IRAS 17179+5444, IRAS 23233+2819 and IRAS 23327+2913 – have stellar masses $M_{\rm stellar} > 1 \times 10^{11}\,{\rm M}_{\odot}$. Although two of these objects – IRAS 1345+132, IRAS 17179+5444 – are spectroscopically classified as Sy2 galaxies in the optical, overall there is no clear-cut distinction between Seyfert and non-Seyfert ULIRGs in terms of their stellar mass; many Seyfert ULIRGs have stellar masses that are relatively modest – at or below the median for the sample as a whole. Thus, our results provide no clear support for the idea that AGN activity in ULIRGs is more likely to be associated with relatively early-type galaxies with massive bulges, as appears to be the case in large samples of galaxies drawn from the Sloan Digital Sky Survey (SDSS) (Heckman et al. 2004; Kauffmann et al. 2004).

In order to compare the results found here with other studies, Table 6 shows the total mass values in units of m_*, defined as the break in the measured mass function obtained from a large sample of 17 173 galaxies drawn from a combination of the Two Micron All Sky Survey (2MASS) Extended Source Catalogue and the Two-Degree Field (2dF) galaxy redshift survey ($m_* = 1.4 \times 10^{11}\,{\rm M}_{\odot}$; Cole et al. 2001 adapted to our cosmology). For the ES sample as a whole, the stellar masses are in the range of $0.1\ m_* \leq M_{\rm stellar} \leq 3.6\ m_*$, with a mean value of $0.6\ m_*$ and a median of $0.4\ m_*$. Approximately 80 per cent of the objects in the ES (27) have total stellar masses $M_{\rm stellar} < 1 \times 10^{11}\,{\rm M}_{\odot}$ ($0.71\ m_*$). Also shown in the table are the dynamical mass estimates (including stars, gas and dark matter) from Tacconi et al. (2002), Colina et al. (2005) and Dasyra et al. (2006a,b) for the objects in common with the ES. The values presented in the table are for the entire systems, including the extended regions of the galaxies and adding the dynamical masses of the two nuclei for the double nucleus systems. To measure the dynamical masses of the systems, Tacconi et al. (2002) and Dasyra et al. (2006a,b) used near-IR CO and Si I absorption features, tracing the stars in the galaxies, although Dasyra et al. (2006a,b) also used the [Fe II] forbidden emission line, which is a tracer of the warm, ionized gas. In contrast, Colina et al. (2005) used the optical Hα emission line, which also traces the warm, ionized gas. The main uncertainties associated with these techniques are: (1) the internal extinction; (2) the light contribution from AGN and/or compact, nuclear starburst; and (3) the assumption of virialization (for a detailed discussion see Colina et al. 2005). A comparison between our modelling results and those of the kinematical studies mentioned above shows that:

(i) typically the stellar masses are within a factor of ∼2 of the dynamical masses, which is remarkable given the uncertainties in both spectroscopic and dynamical techniques;

(ii) the dynamical masses tend to be larger than the stellar masses in most cases. However, this is not surprising given that the dynamical masses account for all the mass (including stars, gas and dark

Table 6. Estimated total masses associated with the stellar populations (YSPs, including VYSPs and IYSPs, and OSPs if present) detected at optical wavelengths, expressed in units of m_* ($m_* = 1.4 \times 10^{11}\,{\rm M}_{\odot}$). Due to the powerful AGN emission, it was not possible to estimate the total mass for the three objects in our sample classified as Sy1 galaxies (IRAS 12540−5708, IRAS 15462−0405 and IRAS 21219−1757).

Object name IRAS	$M_{\rm stellar}$ (m_*)	$M_{\rm dyn}{}^a$ (m_*)	$M_{\rm dyn}{}^b$ (m_*)	$M_{\rm dyn}{}^c$ (m_*)
00091–0738	0.33	...	...	...
00188–0856	0.72	...	...	...
01004–2237	0.11	...	...	0.07
08572+3915	0.20	...	0.13	...
10190+1322	0.28	...	...	0.93
10494+4424	0.37	...	...	...
12072–0444	0.26	...	...	...
12112+0305	0.52	...	0.70	0.40
12540+5708	...	...	...	...
13305–1739	0.28	...	...	...
13428+5608	0.53	2.0	0.6 - 1.1	0.88
13451+1232	3.60	...	...	...
13539+2920	0.24	...	...	...
14060+2919	0.40	...	...	...
14252–1550	0.38	...	...	...
14348–1447	0.77	1.0	1.1	1.50
14394+5332	0.44	...	...	...
15130–1958	0.28	...	...	0.51
15206+3342	0.60	...	0.3	...
15327+2340	0.25	0.3	0.3	0.26
16156+0146	0.22	...	...	...
16474+3430	0.61	...	...	...
16487+5447	0.67	...	...	...
17028+5817	0.40	...	...	...
17044+6720	0.19	...	...	...
17179+5444	1.24	...	...	...
20414−1651	0.25	...	...	0.52
21208–0519	0.68	...	...	...
22491–1808	0.20	...	...	0.68
23060+0505	0.49	...	...	...
23233+2817	1.64	...	...	...
23234+0946	0.34	...	...	...
23327+2913	3.37	...	...	...
23389+0303	0.15	...	...	...

[a]Dynamical mass from Tacconi et al. (2002).
[b]Dynamical mass from Colina et al. (2005).
[c]Dynamical mass from Dasyra et al. (2006a,b).

matter), whereas the spectroscopic masses only account for the stars.

The results presented here reinforce the idea that ULIRGs are sub-m_* or $\sim m_*$ systems (Genzel et al. 2001; Tacconi et al. 2002; Colina et al. 2005; Dasyra et al. 2006a,b). They also provide evidence that the optically visible stellar populations dominate the stellar masses of the systems; the mass contributions of any stellar populations entirely hidden by dust must be relatively minor.

4 BOLOMETRIC LUMINOSITIES: HIDDEN STARBURST COMPONENTS

As well as the total stellar masses, the estimated values for the bolometric luminosities associated with the stellar populations detected at optical wavelengths are also presented in Table 4, of Paper I. For the ES, we find a mean value of $L_{\rm bol} = 0.66 \times 10^{12}\,{\rm L}_{\odot}$ and a median of $L_{\rm bol} = 0.53 \times 10^{12}\,{\rm L}_{\odot}$. Assuming that most of the optical light is absorbed and reprocessed by dust, it is interesting to compare these values with the MFIR luminosities of the sources. Fig. 5 presents a histogram showing the estimated stellar bolometric luminosities of the YSPs detected in the optical expressed as percentages of the MFIR luminosities of the 33 sources in the ES considered here (all but the three Sy1, for which it was not possible to estimate $L_{\rm bol}$). We find that for 48 per cent of the objects (16 of 33) the bolometric luminosities of the YSPs detected at optical wavelengths represent a large fraction ($\gtrsim$ 50 per cent) of the mid- to far-IR luminosities of the sources.

However, note that six of the 16 objects in which $L_{\rm bol}$(YSP) represents a large fraction of the $L_{\rm IR}$ are spectroscopically classified as Sy2 galaxies in the optical. Due to potential AGN contamination, the contribution of the stellar populations to the optical light, and therefore the bolometric luminosity associated with them, is less well constrained for these objects than for the other ULIRGs. Hence, it is possible that the true values of the stellar bolometric luminosities presented in Paper I are significantly smaller. Excluding these six objects from the group of 16, we find that in 23 of the remaining 33 objects in the ES (70 per cent) the bolometric luminosities of the YSPs represent only a modest fraction of mid- to far-IR luminosities ($L_{\rm ysp}/L_{\rm ir} < 0.5$). On the other hand, there remain 10 objects in the ES (∼30 per cent), with no evidence of AGN activity, for which we find that the YSP luminosities represent a large proportion of their MFIR luminosities.

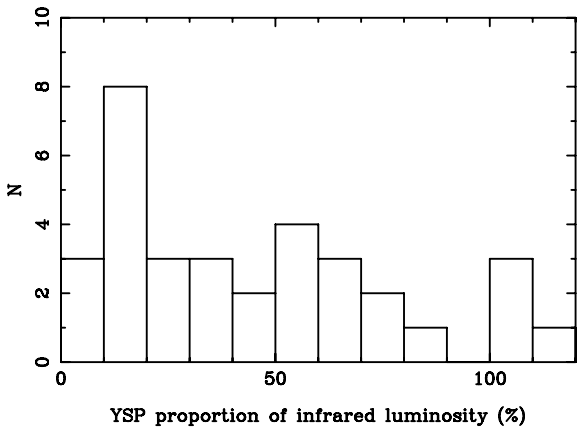

Figure 5. Histogram showing the estimated bolometric luminosities of the YSPs detected in the optical expressed as percentages of the mid- to far-IR luminosities of the 33 sources in the ES considered here.

At this stage, it is important to mention that there are two major uncertainties associated to the results presented in this section: first, uncertainties in the selection of a particular model that is then applied to the whole galaxy; secondly, the assumption that all the stellar light is actually absorbed by, and heats the dust that radiates at mid- to far-IR wavelengths. In the former case, our model selection and assumptions are unlikely be substantially in error, since the stellar masses derived from the same models compare well with the dynamical masses. Of more concern is the second assumption: that all the light from the stellar populations is absorbed by, and heats the dust. In at least some cases, the reddening of the VYSP in the nuclear aperture is fairly modest (see Paper I for details) and the IYSP reddening is constrained to be $E(B-V) \leq 0.4$. In the extended regions not covered by the slit (but included in our bolometric luminosity estimates because of the aperture correction of the flux), the reddening is likely to be even less. Therefore, it is possible that a substantial fraction of the starlight from the stellar populations detected in the optical escapes each galaxy, and that the stellar bolometric luminosities presented in table 10 in Paper I and Fig. 5 in this paper represent overestimates of the ability of the starlight to heat the dust.

5 THE NATURE OF THE PROGENITOR GALAXIES

We discuss in this section the extent to which the stellar populations detected in the optical have been formed during the merger, and also the nature of the progenitor galaxies involved in the triggering events. The aim is to answer two simple, but important, questions. First, are the YSPs detected in optical observations of ULIRGS all formed during the merger event? Secondly, can we use studies similar to that presented here in order to determine the SF histories in major galaxy mergers?

As outlined by RZ08, the contamination by YSPs present in the discs of the galaxies prior to the merger is potentially an important issue. We investigate this by comparing the VYSPs masses of late-type spirals, likely progenitors of ULIRGs, with those of the IYSPs in the ULIRGs in our ES. The reason to focus on the VYSPs in spirals is that, if the SF is truncated during the merger, these are the stellar populations that may evolve into the IYSPs observed today. For the ULIRGs in the ES, we obtain IYSP masses in the range $M_{\rm IYSP} = 0.5\text{–}50 \times 10^{10}\,{\rm M}_{\odot}$, with a mean value of $6.0 \times 10^{10}\,{\rm M}_{\odot}$ and a median of $3.4 \times 10^{10}\,{\rm M}_{\odot}$ (see Paper I). In comparison, RZ08 estimated that the VYSP of typical late-type (Sc) spiral galaxies have VYSP masses in the range $M_{\rm VYSP}({\rm Sc}) = 1.2\text{–}\,8.5 \times 10^{9}\,{\rm M}_{\odot}$. Therefore, it is clear that, assuming an equal mass merger, both of the progenitor spiral galaxies must be at the upper end of the mass range in order to explain the IYSPs in ULIRGs in terms of VYSP from the captured discs of the progenitor galaxies; clearly, the ULIRGs with the more massive IYSPs would be difficult to explain in this way.

Alternatively, we can consider the nature of the progenitor galaxies that would be required to produce the YSP (IYSP and VYSP) and gas masses of ULIRGs by gas-rich mergers. In this case we assume that the YSPs were formed entirely by merger-induced SF. The total gas masses $M({\rm H_2 + H\,I})$ of ULIRGs are typically of order a few times $10^{10}\,{\rm M}_{\odot}$ (Mirabel & Sanders 1988; Solomon et al. 1997; Evans et al. 2002). Adding these gas masses to the total masses of the IYSP and VYSP (from table 4 in Paper I), which we are assuming have formed in the mergers, we find a total mass

$M(\mathrm{gas}+\mathrm{YSP}) > 5 \times 10^{10}\,\mathrm{M}_{\odot}$ in many of the objects in our sample. Given that the merger-induced SF is unlikely to be more than 50 per cent efficient, the progenitor galaxies are together required to have an even larger gas mass. In comparison, using the compilation of H I masses in Roberts & Haynes (1994), and assuming an H_2/H I ratio of 0.7 for spirals (Young & Knezek 1989), we find that typical late-type (Sc) spiral galaxies have total gas masses of $M(\mathrm{H_2}+\mathrm{H\,I}) \sim 1.4 \times 10^{10}\,\mathrm{M}_{\odot}$ (see RZ08 for details). Therefore, the progenitor galaxies are required to be at the upper end of the mass range for late-type spirals to explain the total YSP and gas masses of the ULIRGs. Note that, even if we consider only the gas masses, we require two 'average' late-type spiral galaxies to merge in order to produce the typical gas masses measured in ULIRGs, and this is without accounting for any losses of gas due to outflows and SF in the merger.

Finally we note that 33 per cent of the objects in the ES have VYSPs with masses $M_{\mathrm{VYSP}} \gtrsim 10^{10}\,\mathrm{M}_{\odot}$ (see Paper I). Since these VYSP must be formed during the merger, and the SF efficiency is likely to be <50 per cent, the total amount of gas required in the progenitor galaxies is much larger; again a merger of two late-type spirals of average or larger mass would be required to produce the VYSP alone in these systems.

At this stage, it is important to add a caveat about the nature of the progenitor galaxies. It is commonly accepted that the ULIRG phenomenon is associated with gas-rich mergers in which both galaxies are spiral galaxies. This is supported by the mass arguments presented above, as well as the lack of evidence for a major contribution from an OSP in most of the ULIRG sample. However, in the cases of one of the nuclear apertures in each of the double nucleus systems IRAS 21208−0519 and IRAS 23327+2913, adequate fits are only obtained with a combination of stellar populations that includes a dominant contribution of a 12.5 Gyr OSP, plus a VYSP. Overall, these results suggest that mergers in which at least one of the progenitors had an early-type morphology can also trigger the ULIRG phenomenon.

6 COMPARISON WITH MERGER MODELS

The range of different morphologies of the objects in the ES, from widely separated double nuclei systems (e.g. IRAS 14394+5332) to single nucleus galaxies with no strong signs of tidal structures (e.g. IRAS 15206−3342), suggests a variety of different stages of merger events. In this section, we give an overview of how our modelling results fit in with the merger simulation predictions.

In general terms, the simulations predict two epochs of starburst activity (Barnes & Hernquist 1996; Mihos & Hernquist 1996; Springel et al. 2005) in major gas-rich mergers: the first occurring around or just after the first peri-centre passage, and a second more intense episode towards the end of the merger, ∼0.5–1.5 Gyr after the first peri-centre passage, when the nuclei are close to coalescing (within $\sim 5 \times 10^7$ Myr of coalescence). However, both the time lag and the relative intensity of the peaks of starburst activity during the merger event depend on several factors, such as: the presence of bulges, feedback effects, gas content and orbital geometry. For example, the presence of a bulge acts as a stabilizer of the gas against inflows and the formation of bar structures, allowing stronger starburst activity towards the end of the merger event (Barnes & Hernquist 1996; Mihos & Hernquist 1996). On the other hand, AGN feedback effects (e.g. quasar-driven winds) disrupt the gas surrounding the black hole, acting against the SF activity at all stages (Springel et al. 2005).

In Paper I, we showed that it is possible to model all of the extracted spectra with a combination of two stellar populations, plus a power law in some cases. Concentrating again on Combination III, the modelling results are, in general terms, consistent with the merger simulations. For example, it is possible that the IYSPs detected in most apertures are related to the first enhancement of the starburst activity, around or just after the time of the first peri-centre passage, and we are now seeing the objects at a later stage.

We emphasize that, although the VYSPs are more significant in the nuclear regions of the galaxies, this component is detected at all locations sampled by the extended apertures for the overwhelming majority of the objects. We also find a trend for the VYSPs in the nuclear regions to be younger and more reddened than those of the extended regions. All of these results are consistent with the merger simulations, which predict that the SF activity in the final stages of merger is concentrated towards the nuclear regions of the merging galaxies, coinciding with higher concentrations of gas and dust, but it also occurs within the tidal structures formed during the interaction. Furthermore, as described in Section 2, when using Combination I, we find a clear cut-off in YSP ages at 100 Myr in the nuclear regions. This is in good agreement with the time-scale (≤100 Myr) of the induced starburst activity predicted by the theoretical models for the final stages of a merger, as the nuclei coalesce (Mihos & Hernquist 1996; Springel et al. 2005).

We note that ongoing SF activity is also detected for all objects with relatively wide nuclear separations: IRAS 14394+5332[3] (54 kpc), IRAS 17028+5817 (25 kpc), IRAS 21208−0519 (15 kpc) and IRAS 23327+2913 (24 kpc). Three of these objects, IRAS 17028+5817, IRAS 21208−0519 and IRAS 23327+2913, show no signs of AGN activity. SF rates of $\mathrm{SFR} \gtrsim 170\,\mathrm{M}_{\odot}\,\mathrm{yr}^{-1}$ are required in order to produce the IR luminosities ($L_{\mathrm{IR}} \geq 10^{12}\,\mathrm{L}_{\odot}$) in these latter objects (Kennicutt 1998). As noted above, such high SF rates are only predicted by the merger simulations in two stages during the merger event:

(i) at, or after, the first peri-centre passage, if the parent galaxies have insignificant bulges and feedback effects are not important, or

(ii) at the end of the merger event, close (within ∼50 Myr) to the coalescence of the nuclei.

Estimates of the dynamical time-scales for completion of the mergers range from ≥50 Myr in the case of IRAS 21208−0519, to ≥80 Myr in the cases of IRAS 17028+5817 and IRAS 23327+2913[4] Therefore, if the SF activity is associated with the final starburst that occurs around the time of the coalescence of the nuclei, then this starburst must be relatively long-lived in these three wide separation systems. Alternatively, the enhanced SF activity in these systems may be associated with the (relatively extended) period of SF that follows as the galaxies move apart after the first peri-centre passage of the two nuclei. However, for the latter case, the existing merger simulations do not predict the large SF rates ($\gtrsim 100\,\mathrm{M}_{\odot}\,\mathrm{yr}^{-1}$) for the extended period after the first encounter, that would be required for these systems to be observed as ULIRGs. Most probably, these wide nuclear separation ULIRGs are systems

[3] Note that in the case of IRAS 14394+5332, the widest separation system in the sample, the ULIRG phenomenon is not related with the interaction of the two widely separated systems, but with the eastern source, which is itself a merger in its final stages.

[4] In making these dynamical time-scale estimates, we have assumed that the projected distances between the nuclei represent their true separation, and that the nuclei are moving radially towards each other with a relative radial velocity of 300 km s^{-1}.

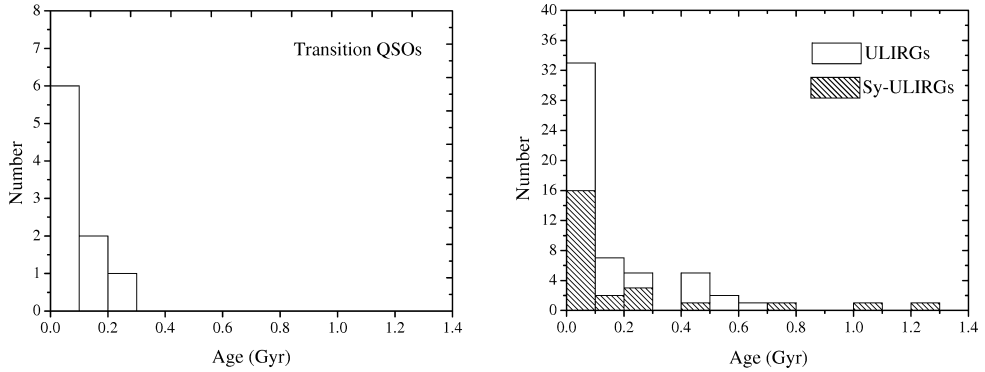

Figure 6. The young stellar age distribution for the Canalizo & Stockton (2001) transition QSOs (left-hand panel) and the extended regions of the ULIRGs in the ES (right-hand panel), with Seyfert ULIRGs highlighted. These results are based on modelling Combination I. It is clear that the transition QSOs, Seyfert ULIRGs and non-Seyfert ULIRGs overlap in terms of their distributions of YSP ages in these diagrams.

in which the final starburst has been triggered relatively early in the period prior to coalescence, as the nuclei move together in the final stages of the merger.

7 EVOLUTIONARY SCENARIOS

The presence of evolutionary links between ULIRGs, QSOs/radio galaxies and elliptical galaxies is commonly accepted. However, the true nature of the links remain uncertain. While some authors propose the evolutionary sequence cool ULIRG → warm ULIRG → optically selected QSO or radio galaxy (Sanders et al. 1988a; Canalizo & Stockton 2001), other authors (Genzel et al. 2001; Tacconi et al. 2002) dismiss such an evolutionary sequence based on the location of ULIRGs in the fundamental plane, similar to that of the intermediate mass ($\sim L_*$) elliptical galaxies. We will compare here our study of a sample of 36 ULIRGs with studies of the stellar populations in samples of QSOs and related objects.

Canalizo & Stockton (2000a,b, 2001) carried out a similar study to that presented here for their sample of nine 'transition QSOs' – objects that may represent a transitionary stage between ULIRGs and QSOs. All of their sample objects show clear signs of interaction, and five of them are classified as major mergers. Furthermore, all but one have IR luminosities $L_{\rm IR} \geq 10^{12}\,{\rm L}_{\odot}$ (i.e. they are ULIRGs). In order to study a possible link between these objects and the general populations of ULIRGs, Canalizo & Stockton investigated the stellar populations within the host galaxies. For that purpose, they modelled the optical spectra extracted from a series of extended apertures using a combination of a 10 Gyr OSP plus YSPs with varying ages, which is similar to the Combination I used here.

Fig. 6 presents histograms comparing the distribution of the YSP ages derived by Canalizo & Stockton (2000a,b, 2001) for the transition QSOs, with those obtained for the ULIRGs in the ES sample using Combination I (labelled as LW age in Section 3). For the transition QSOs, we have used the starburst peak ages (Canalizo & Stockton 2001, column 5 of their table 3), defined as the predominant starburst age found in the host galaxy (see Canalizo & Stockton 1997, 2000a,b, for details), while for the ULIRGs we have used the average values of the LW age, i.e. the same as in Fig. 1. Note that, since the nuclear regions could not be sampled due to contamination by the bright quasar nuclei, the Canalizo & Stockton studies concentrate on the extended regions of the objects. Therefore, we have compared their results with those for the extended regions of the ULIRGs in the ES. Fig. 6 also shows the results obtained in this study for the extended apertures of the Sy-ULIRGs (the 'oldest' ages in this figure are obtained for the atypical object PKS 1345+12).

As described in Section 2, we do not find any significant differences between the ages obtained for the H II- and LINER-ULIRGs and those of the Sy-ULIRGs in the ES. The same conclusions are reached if we compare the transition QSOs with the Sy-ULIRGs in the ES sample, or with the sample of ULIRGs as a whole. If there is an evolutionary link between ULIRGs as a class and the transition QSOs, one would expect the latter to have, in general, older YSP ages than ULIRGs, although some overlap is expected. However, it is clear from the figure that the ages obtained for the extended apertures in the transition QSOs are very similar to those of the extended apertures of the ULIRGs in the ES. A first interpretation of this result is that there is no clear evolutionary link between non-Seyfert ULIRGs and transition QSOs. However, as mentioned in Section 2, it is possible that the time-scale for the transition from ULIRGs to QSOs is smaller than the time-scale associated with the ULIRG phenomenon.

Therefore, our study does not provide any clear-cut evidence for an evolutionary link between ULIRGs and the QSOs. Certainly, it is unlikely that the AGN in the Seyfert ULIRGs in our sample have been triggered a substantial period (>100 Myr) *after* the main merger-induced starburst, as appears to be the case in some radio galaxies (Tadhunter et al. 2005; Wills et al. 2008).

8 COMPARISON WITH STUDIES OF HIGH-*Z* OBJECTS

Star-forming galaxies have been detected in large numbers at high redshifts ($z \gtrsim 1$). These galaxies are selected on the basis of their strong UV emission (Lyman-break galaxies – LBGs: see Giavalisco 2002, for review), high sub-mm luminosities (SMGs; Blain et al. 2002; Smail et al. 2002; Chapman et al. 2003; Pope et al. 2005) mid-IR flux densities (24 μm *Spitzer*-selected galaxies,[5] Papovich et al. 2004; Caputi et al. 2006; Sajina et al. 2007; Yan et al. 2007; Farrah

[5] Note that within the so-called 24 μm *Spitzer*-selected galaxies class, there will be galaxies classified as LBGs, SMGs and DRGs. However, not all LBGs and/or DRGs will be detected at 24 μm and, therefore, we refer to the 24 μm *Spitzer*-selected objects as a class of galaxies with their own properties.

Table 7. The stellar masses of the different types of high-z star-forming galaxies found in different studies. The stellar masses for the ULIRGs found in this study are also shown in the table for comparison. Note that the upper limit of 50×10^{10} M$_\odot$ is found for the radio galaxy PKS 1345+12, which represents an exceptional case among the ULIRGs in our sample. All results obtained for the high-z star-forming galaxies are based on the modelling of photometric points from the optical to the mid-IR.

Star-forming galaxy type	$M_{\rm stellar}$ 10^{10} M$_\odot$	References
Lyman-break	0.2–6.0	Papovich et al. (2001)
Sub-mm	12–25	Tacconi et al. (2008)
Distant red	2.9–46.0	Papovich et al. (2006)
24 μm *Spitzer*	0.1–100	Caputi et al. (2006)
Local ULIRGs	0.2–50.0	This work

et al. 2008), or red near-IR colours: $(J - K)_{\rm vega} \gtrsim 2.3$ (DRGs; Franx et al. 2003). A large fraction show morphological features suggesting that major mergers are common among such objects (Giavalisco 2002; Chapman et al. 2003; Erb et al. 2003, 2004; Conselice, Blackburne & Papovich 2005). In addition, Frayer et al. (2004), based on deep near-IR imaging, concluded that the colours, luminosities, morphologies and sizes of the SMGs in their sample are all consistent with the properties of local ULIRGs. Furthermore, on the basis of their CO millimetre observations, Tacconi et al. (2006) conclude that SMGs appear to represent 'scaled-up' version of local ULIRGs. Therefore, it is interesting to compare the results of this study with those obtained for high-z star-forming galaxies.

Table 7 shows a compilations of the results obtained from various studies of the stellar masses of high-z star-forming galaxies. We find that the masses of the local ULIRGs in our sample are, in general, comparable with or slightly higher than, those of the LBGs in the Papovich, Dickinson & Ferguson (2001) sample. In the case of the DRGs, the results found by Papovich et al. (2006) are consistent with the total stellar mass estimated in this work for local ULIRGs, and reinforce the idea that the latter objects are the low-redshift analogues of the DRGs found at higher redshifts. On the other hand, we find that the estimated stellar masses for the ULIRGs in our sample are significantly smaller (with the exception of the radio galaxy PKS12345+12) than many of the SMGs and the *Spitzer* galaxies. This result is consistent with those of the recent studies of, for example, Sajina et al. (2007, 2008), Yan et al. (2007), Farrah et al. (2008), Rigby et al. (2008) and Tacconi et al. (2008) among others, suggesting that the SMGs and the *Spitzer* galaxies are either maximum starburst, i.e. scaled-up versions of local ULIRGs, or indeed represent a separate class of objects from local ULIRGs.

Finally, note that the results obtained for the stellar populations of high-z star-forming galaxies are based on fits to relatively few photometric points, albeit with a wide spectral range. The modelling work detailed in Paper I emphasized the difficulty in obtaining a unique solution when using combinations of different stellar populations to model spectra, especially on the basis of fits to the SED alone (i.e. not examining the detailed absorption features). We have also shown that some results, and therefore the conclusions based on them, can change significantly with different modelling assumptions. Furthermore, the SED fits for DRGs in the Papovich et al. (2006) sample are relatively poor ($\chi^2_{\rm red} \gtrsim 2$) in a large fraction ($\gtrsim$50 per cent) of the sources. Such poor fits would not be accepted as viable in our study of ULIRGs. Clearly, particular care must be taken when interpreting the results obtained on the basis of modelling a few photometric points using combinations of stellar templates, which is often the technique used in high-z studies. Studies similar to the one presented here are vital for increasing our understanding, not only of the properties of the stellar populations in high-z star-forming galaxies, but also the nature of the links between these objects and the local ULIRGs.

9 SUMMARY AND CONCLUSIONS

In this paper, we have presented a detailed analysis of the modelling results presented for the CS and the ES samples in Paper I. In addition, we have also discussed these results in a more general context, comparing them with other studies of ULIRGs. The conclusions can be summarized as follows.

(i) *Age, reddening and percentage contribution*. We find that the YSPs are more significant in the nuclear than in the extended regions. The statistical analysis presented here suggests that the YSPs located in the nuclear regions tend to be younger and more reddened, although further analysis is required to confirm this result. All of these results are consistent with the merger simulations.

(ii) *Correlations*. We find no evidence for correlations between the properties of the stellar populations and other properties of ULIRGs. This can be explained in terms of a selection effect, i.e. since the objects in the CS and the ES samples are ULIRGs, with high IR luminosities and SF rates, it is likely that we are observing them at, or after, the first peri-centre passage, or at the end of the merger event, when the nuclei are very close to coalescing. Therefore, they all have similar properties. A second possibility to explain the apparent lack of correlations is the scatter in the properties of the YSPs due to uncertainties in the modelling technique. A third possible explanation is that other variables, such as gas content of the parent galaxies and the geometry of the collision, may have a more important impact on the stellar properties of ULIRGs than the optical spectral classification, interaction class or luminosity.

(iii) *Merger simulations*. In general, our modelling results are consistent with the merger simulations, with the IYSPs in most systems plausibly associated with the first enhancement of activity following the first peri-centre passage of the nuclei of the merging galaxies, and the VYSPs likely related to the final enhancement of the SF as the nuclei merge together.

(iv) *100 Myr cut-off*. When using Combination I, we find a clear cut-off in LW YSP ages at 100 Myr for the nuclear apertures, consistent with the time-scale of the merger-induced starburst activity predicted by the merger simulations in the final stages of the merger event, as the nuclei coalesce. This result supports the idea that, despite the varying morphologies, we are observing most of the objects close to the peak of the SF activity in the final stages of the merger event.

(v) *The masses of the parent galaxies*. Both progenitor galaxies in the triggering merger must be in the upper 25 per cent of the mass range of late-type spirals for most of the ULIRGs in the ES.

(vi) *The morphologies of the parent galaxies*. Although in most cases the results are consistent with the idea that the progenitors are late-type spirals (albeit unusually massive late-type spirals), in three cases (IRAS 13451+1232, IRAS 21208−0519 and IRAS 23327+2913) there is clear evidence that at least one of the progenitors is an early-type galaxy. This demonstrates that ULIRGs can potentially be triggered by mergers between galaxies with a range of galaxy types.

(vii) *Stellar mass content*. Our modelling results suggest that most ULIRGs are sub-m_*, or m_* systems ($m_* = 1.4 \times 10^{11}\,M_\odot$). Such masses support the idea that these systems will eventually evolve into intermediate mass elliptical galaxies. The masses obtained from the modelling results are generally consistent with the dynamical mass estimates (when available) within a factor of $\sim$2. This result shows that the stellar populations detected in the optical dominate the stellar masses of the galaxies.

(viii) *Bolometric luminosities.* Our results suggest that the stellar populations detected at optical wavelengths make a significant contribution to the mid- to far-IR luminosities of many of the sources. However, due to uncertainties related to the combination of stellar populations assumed, and to the assumption that all the stellar emission is absorbed by, and heats, the dust, it is possible that the values presented in table 10 in Paper I and Fig. 5 in this paper are overestimates. We conclude that while the visible stellar populations can make a significant contribution to the heating of the dust, it is unlikely that they dominate the heating of the dust in most cases.

(ix) *The evolution of ULIRGs*. The stellar masses of the ULIRGs in the ES sample are consistent with the idea that ULIRGs evolve into intermediate mass elliptical galaxies. On the other hand, the data do not provide any clear evidence to support/refute the evolutionary sequence: cool ULIRG $\rightarrow$ warm ULIRG $\rightarrow$ optically selected QSO, since the stellar populations of the cold/warm, Sy/non-Sy, QSO/non-QSO ULIRGs are similar (perhaps the time-scale of this transition is shorter than the time-scale of the major merger-induced starburst). However, it remains possible that some ULIRGs evolve into radio galaxies (although not all radio galaxies can have this origin).

(x) *High-z counterparts*. Many of the properties of the ULIRGs in our sample, such as morphology, stellar mass content, SF histories, etc., are consistent with the idea that ULIRGs are the local counterparts of the SMGs and DRGs.

ACKNOWLEDGMENTS

We thank the anonymous referee for useful comments that have helped to improve this manuscript. JRZ acknowledges financial support from the STFC in the form of a PhD studentship. JRZ also acknowledges financial support from the spanish grant ESP2007-65475-C02-01. RGD is supported by the Spanish Ministerio de Educación y Ciencia under grant AYA 2007-64712. We also thank support for a joint CSIC-Royal Astronomy Society bilateral collaboration grant. The William Herschel Telescope is operated on the island of La Palma by the Isaac Newton Group in the Spanish Observatorio del Roque de los Muchachos of the Instituto de Astrofísica de Canarias.

REFERENCES

Barnes J., Hernquist L., 1996, ApJ., 471, 115
Blain A. W., Smail I., Ivison R. J., Kneib J.-P., Frayer D. T., 2002, Phys. Rep., 369, 111
Canalizo G., Stockton A., 1997, ApJ, 490, L5
Canalizo G., Stockton A., 2000a, AJ, 528, 201
Canalizo G., Stockton A., 2000b, AJ, 120, 1750
Canalizo G., Stockton A., 2001, ApJ, 555, 719
Caputi K. I. et al., 2006, ApJ, 637, 727
Chapman S. C., Windhorst R., Odewahn S., Yan H., Conselice C., 2003, ApJ, 599, 92
Cole S. et al., 2001, MNRAS, 326, 255
Colina L., Arribas S., Monreal-Ibero A., 2005, ApJ, 621, 725
Conselice C. J., Blackburne J. A., Papovich C., 2005, ApJ, 620, 564
Cox T. J., Jonsson P., Primack J. R., Somerville R. S., 2006, MNRAS, 373, 1013
Cox T. J., Jonsson P., Somerville R. S., Primack J. R., Dekel A., 2008, MNRAS, 384, 386
Dasyra K. et al., 2006a, ApJ, 638, 745
Dasyra K. et al., 2006b, ApJ, 651, 835
Dasyra K. M. et al., 2007, ApJ, 657, 102
di Matteo P., Combes F., Melchior A.-L., Semelin B., 2007, A&A, 468, 61
Erb D. K., Shapley A. E., Steidel C. C., Pettini M., Adelberger K. L., Hunt M. P., Moorwood A. F. M., Cuby J.-G., 2003, ApJ, 591, 101
Erb D. K., Steidel C. C., Shapley A. E., Pettini M., Adelberger K. L., 2004, ApJ, 612, 122
Evans A., Mazzarella J., Surace J., Sanders D., 2002, AJ, 580, 749
Farrah D. et al., 2001, MNRAS, 326, 1333
Farrah D., Afonso J., Efstathiou A., Rowan-Robinson M., Fox M., Clements D., 2003, MNRAS, 343, 585
Farrah D. et al., 2008, ApJ, 677, 957
Franx M. et al., 2003, ApJ, 587, L79
Frayer D. T., Reddy N. A., Armus L., Blain A. W., Scoville N. Z., Smail I., 2004, AJ, 127, 728
Genzel R., Tacconi L. J., Rigopoulou D., Lutz D., Tecza M., 2001, ApJ, 563, 527
Giavalisco M., 2002, ARA&A, 40, 579
Heckman T. M., Kauffmann G., Brinchmann J., Charlot S., Tremonti C., White S. D. M., 2004, ApJ, 613, 109
Kauffmann G., White S. D. M., Heckman T. M., Ménard B., Brinchmann J., Charlot S., Tremonti C., Brinkmann J., 2004, MNRAS, 353, 713
Kennicutt R., 1998, ARA&A, 36, 189
Kim D. C., Sanders D. B., 1998, ApJ, 119, 41
Mihos J., Hernquist L., 1996, ApJ, 464, 641
Mirabel I., Sanders D., 1988, ApJ, 355, 104
Papovich C., Dickinson M., Ferguson H. C., 2001, ApJ, 559, 620
Papovich C. et al., 2004, ApJS, 154, 70
Papovich C. et al., 2006, ApJ, 640, 92
Pérez-González P. G. et al., 2005, ApJ, 630, 82
Pope A., Borys C., Scott D., Conselice C., Dickinson M., Mobasher B., 2005, MNRAS, 358, 149
Rigby J. R. et al., 2008, ApJ, 675, 262
Roberts M., Haynes M., 1994, ARA&A, 32, 115
Robinson T., Tadhunter C., Axon D., Robinson A., 2000, MNRAS, 317, 922
Rodríguez Zaurín J., Holt J., Tadhunter C., González Delgado R., 2007, MNRAS, 375, 1133 (RZ07)
Rodríguez Zaurín J., Tadhunter C. N., González Delgado R. M., 2008, MNRAS, 384, 875 (RZ08)
Rodríguez Zaurín J., Tadhunter C. N., González Delgado R. M., 2009, MNRAS, 400, 1139 (Paper I)
Sajina A., Yan L., Armus L., Choi P., Fadda D., Helou G., Spoon H., 2007, ApJ, 664, 713
Sajina A. et al., 2008, ApJ, 683, 659
Sanders D. B., Mirabel I. F., 1996, ARA&A, 34, 749
Sanders D. B., Soifer B. T., Elias J. H., Madore B. F., Matthews K., Neugebauer G., Scoville N. Z., 1988a, ApJ, 325, 74
Sanders D. B., Soifer B. T., Elias J. H., Neugebauer G., Matthews K., 1988b, ApJ, 328, L35
Smail I., Ivison R. J., Blain A. W., Kneib J.-P., 2002, MNRAS, 331, 495
Solomon P., Downes D., Radford S., Barret J., 1997, ApJ, 478, 144
Springel V., Di Mateo T., Hernquist L., 2005, MNRAS, 361, 776
Surace J. A., Sanders D. C., 1999, ApJ, 512, 162
Surace J. A., Sanders D., 2000, ApJ, 120, 604
Surace J. A., Sanders D. B., Vacca W. D.Veilleux S., Mazzarella J. M., 1998, ApJ, 492, 116
Surace J., Sanders D., Evans A., 2000, ApJ, 529, 170
Tacconi L. J., Genzel R., Lutz D., Rigopoulou D., Baker A. J., Iserlohe C., Tecza M., 2002, ApJ, 580, 73
Tacconi L. J. et al., 2006, ApJ, 640, 228
Tacconi L. et al., 2008, ApJ, 680, 246

Tadhunter C., Dickson R., Morganti R., Robinson T., Wills K., Villar-Martin M., Hughes M., 2002, MNRAS, 330, 977
Tadhunter C. N., Robinson T. G., González Delgado R. M., Wills K., Morganti R., 2005, MNRAS, 356, 480
Tadhunter C. et al., 2007, ApJ, 661, L13
Veilleux S., Kim D. C., Sanders D. B., 1999, ApJ, 522, 113
Veilleux S., Kim D. C., Sanders D. B., 2002, ApJS, 143, 315
Wills K. A., Tadhunter C. N., Holt J., González Delgado R. M., Rodríguez-Zaurín J., Morganti R., 2008, MNRAS, 385, 136
Yan L. et al., 2007, ApJ, 658, 778
Young J., Knezek P., 1989, ApJ, 347, L55

This paper has been typeset from a TEX/LATEX file prepared by the author.